

# Management System of Power for Microgrid Connected with Renewable Sources

Prachi Pateriya<sup>1</sup> and Upendra Singh Tomar<sup>2</sup>

M.Tech Scholar, Power System, Vikrant Institute of Technology & Management, Gwalior, India<sup>1</sup>

Assistant Professor, Power System, Vikrant Institute of Technology & Management, Gwalior, India<sup>2</sup>

**Abstract:** *In India more than 70% of population is living in villages, which is a major stock holder for GDP and economic growth of a country. Government of India has introduced many programs for health, education, electricity etc. for improvement of the livelihood of villages and out of these programs rural electrification is a major challenge for Government. The electricity will play an important role in the human life for improving the socio-economic conditions in rural areas.*

*According to census 2011 report in India only 55% of households are using electricity. The major challenges for rural electrification are accessibility due to poor paying capacities of house hold poor reliability of grid due to peak hours demand more than 20% loss in Transmission and distribution poor operation and maintenance of distribution System. In this research, to achieve high reliability of isolated hybrid micro grid in smart villages, the real time power management and power quality solution at source and load w.r.t demand generation and time is proposed. Power management system improves the stability of isolated micro grid by synchronizing the load and source as per the demand in smart villages. It helps to segregate the sensitive load and normal load in Village and provide high priority to sensitive loads. Further the real time optimization solution is proposed based on non-cooperative game theory for improvement of stability and reliability of isolated hybrid micro grid. There are three different algorithms are proposed for scheduling of generation and load demand with real time power management system. For improving the power quality, there are mainly the first approach is load side or source side based on load conditions; this approach is called load conditioning based on power management system. Finally the economic study considered to describe the financial viability of the isolated hybrid micro grid at minimum unit cost for village electrification with renewable energy sources*

**Keywords:** Electricity, hybrid micro grid, power management, socio-economic

## I. INTRODUCTION

Today non-renewable energy sources like coal, oil, gas, etc., are used worldwide to produce electrical energy. Fossil fuel burning generates gases (SO<sub>2</sub>, CO, NO<sub>x</sub>, HC, and CO<sub>2</sub>) that cause environmental pollution. It has been estimated that nearly 80% of atmospheric CO<sub>2</sub> is generated by manmade fossil fuel burning, which is typically 50% due to electric power generation. Fig. 1.1 shows the per capita CO<sub>2</sub> emissions versus population for several selected countries globally, where the horizontal axis shows the population and the vertical axis shows the CO<sub>2</sub> emission per person (in tons/year). The United States has the highest per capita emission globally, and Canada is very close to it. Next in the line is Australia and European nations and Russia and Japan, where the emissions are typically less than 50% of the United States. The total emission of a country given by the rectangle area is significant concerning the global warming problem. Also, these non-renewable energies are becoming costly in the world. So, the world scenario is changing towards the use of renewable sources. It is mentioned that renewable energy resources [3–5], such as hydro, wind, solar, bio fuels, geothermal, wave, and tidal powers, are environmentally clean and abundant in nature, and are therefore receiving extreme emphasis throughout the world. Scientific American recently published a paper by two Stanford University professors [6], which predicts that renewable energies alone (with adequate storage) can supply all the world's energy needs. Another study by the UN IPCC reports that renewable resources can meet 50% of total world energy by 2050. Wind and solar resources heavily dependent on power electronics for conversion and control, are particularly important to complete our growing energy needs and mitigate global warming problems. The global

electricity generation from 2012 to 2040 is shown in Fig. 1.2. In which, electricity generation by solar and wind has been continuously increasing from 2012. So, the world is in an excellent position to get an advantage from the momentum of the global shift towards more solar and wind energy future [7]. In the last few years, the penetration of renewable energy has improved in the grid. It is expected to increase in the future. Renewable energy growth in India is shown in Fig. 1.3. Currently, the penetration level is around 21%, with over 80 GW of renewable energy installed. Renewable energy generation is expected to increase by approximately 14.9% per annum during 2019-2030 [7].

## II. MICROGRID

*“A microgrid consists of a distribution network with DER (PV, fuel cells, microturbine, etc.), energy storage (battery, capacitor, etc.), and loads. This system can be operating autonomously if disconnected or interconnected from the grid. The micro sources operation in the network can provide an advantage to the system performance if correlated and managed efficiently.”*

From the above definitions, a microgrid is a localized grouping of distributed energy resources, loads, and energy storage devices that can be operated in islanding and grid connected mode [13].

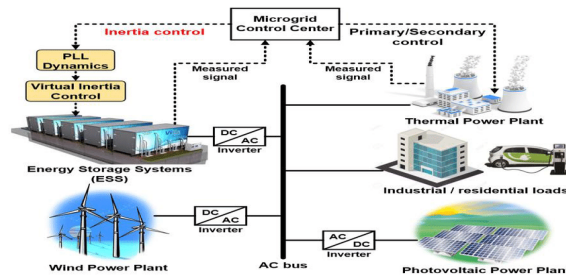


**Figure: Microgrid architecture**

The microgrid is growing rapidly because of its ability to integrate DG. The development of DG has brought as many problems as it has solved for the distribution system. The main problem of the DG is related to the stability and reliability of the distribution system. So, the interconnection of the distributed generators with the distribution system does not create a microgrid. But it must be well controlled with proper control strategies. It gives rise to the concept of local generation and local control of power in a distribution system that is further named as microgrid [14]. The basic diagram of the microgrid is shown in Fig. Microgrids can improve performance, reduce cost, and improve the efficiency of the power system due to reducing transmission & distribution (T&D) losses [14]. The microgrid can benefit both customers and utility [16]. From the utility's view: Microgrid can be seen within the power system as a controlled entity, as a single dispatchable unit (generator or load). From the customer's view: Microgrid is a solution to both electricity and thermal needs, and increase local reliability, decrease emission, better power quality by boost up frequency and voltage and low-cost power supply.

## III. LITERATURE SURVEY

### MICROGRID CONTROL

The MG system is included with three controllers. [26-28].

1. Microgrid Source Controller (MC)
2. Microgrid Central Controller (MGCC) and
3. Load Controller (LC)

The microgrid source controller is connected with each DG unit and energy storage device to flexible and smooth operation to meet customer requirements. The aim of MC is to take care of LC function. It depends on power electronics interfaces. The MC is operated with or without any intervention of MGCC. The MGCC is connected between the microgrid and Distribution Management System (DMS) to optimize the microgrid operation.

### **HIERARCHICAL CONTROL OF MICROGRID**

The multiple sources are connected in parallel with a microgrid bus, which creates issues like bus voltage regulation and power-sharing. Hierarchical control is the best solution to solve such problems. It has various control levels. Even in the centralized controller's failure, it is more reliable to continue the microgrid operation. The microgrid's hierarchical control with its various levels [29-38] is shown in Fig. 2.2.

#### **a. Primary Control:**

It is known as the MC controller. Its preliminary deals with power-sharing among DERs, voltage, and current regulation [39]. It's also avoided circulating current among DERs. The primary controller's function is also for frequency stability, preserving, and plug and play capability of DERs.

#### **b. Secondary Control:**

This controller is appearing on top of the primary controller. It is compensation voltage and frequency deviation caused by primary control [40]. It also deals with system-level like MG synchronization with upper grid, power flow control, power quality regulation, DG coordination, etc.

#### **c. Tertiary Control:**

It is the highest-level control in the hierarchical control architecture of the microgrid. It controls the power flow between the microgrid and the upper grid. The tertiary control conducts forecasting, microgrid supervision, main grid observation, decision-making, system optimization [41], power management [42], economic dispatch [43-45], and energy management [46].

#### **d. Level 0 - Inner control loop:**

It is an inner control loop that finds out the state of DG and the storage device. It is also known as the current and voltage controller [29, 49, 50]. The feedback and feed forward compensators, linear, and non-linear control are also included.

#### **e. Level 1 - Local control loop (Primary Control):**

It is known as the primary control. There is no communication between the DG unit. So, it is also known as decentralized control [51, 52]. The P/Q droop control (active power P-frequency  $f$  control and reactive power Q-voltage V) is included in this control loop [34, 53].

#### **f. Level 2 - Secondary control loop:**

The microgrid central controller (MGCC) is located at this level. It measures voltage and frequency [50, 54, 55]. After comparing reference value, deviation of voltage and frequency are generated by this control loop. It regulates the voltage and frequency of the microgrid. The synchronization control and main grid connection with the microgrid are also included. [51]

#### **g. Level 3 - Global control loop (Tertiary Control):**

It is also known as tertiary control of microgrid. In this control, the energy market or production stage controls the power flow between the grid and microgrid [29, 56]. When the microgrid is connected to the central grid system, the power flow is controlled by the inside voltage.

## **IV. RESULTS**

The presence of DG characterizes the microgrid. The renewable sources PV and wind are used as DG in a proposed hybrid microgrid. In this chapter, PVES, WES, and Energy storage systems are illustrated. In PVES and WES, the modeling of PV and PMSG are analyzed. The role of MPPT is important in PVES and WES because it extracts the maximum output of sources and maximizes the efficiency of the system. The MPPT control in PVES and WES at variable irradiance and wind speed are found in MATLAB/Simulink.

### **Modeling and Control of PVES**

The PV energy system is the largest energy source to produce electrical power and the fastest building up electrical power generation globally. The modeling of a PV system can be analyzed by interfacing the PV system to the boost converter, load, and the tracking of the maximum power point of PV. The PV cell's fundamental modeling by its an equivalent circuit, PV characteristics, MPPT, and simulation of PVES with MPPT control are discussed.

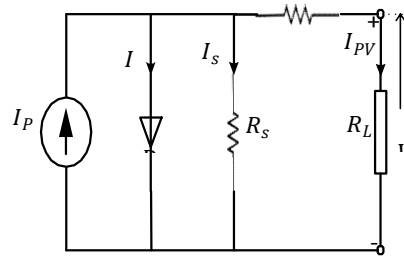


**FIGURE: Equivalent circuit of PV Solar Cell**

**TABLE: PV Module -TGD Holding T250M606 data at STC**

Parameter	Rating
Maximum power [ $P_{max}$ ]	250.205 W
Current at Maximum Power Point (MPP) [ $I_{mpp}$ ]	8.15 A
Voltage at Maximum Power Point (MPP) [ $V_{mpp}$ ]	50.7 V
Short Circuit (SC) current [ $I_{sc}$ ]	8.8 A
Open Circuit (OC) voltage [ $V_{oc}$ ]	58.1 V
Cell per module	60
Temperature coefficient of [ $I_{sc}$ ]	0.017 (%/deg. C)
Temperature coefficient of [ $V_{oc}$ ]	-0.58059 (%/deg. C)
Light generated current [ $I_L$ ]	8.8179 A
Diode saturation current [ $I_0$ ]	$5.5524 e^{-10}$ A
Diode ideality factor	1.0555

**TABLE: Specification of PV Array using TGD Holding T250M606**

Parameter	Rating
No. of modules connected in a series string [ $N_{ser}$ ]	8
No. of modules connected in parallel string [ $N_{par}$ ]	5
Maximum power [ $P_{max}$ ]	10 KW
Current at Maximum Power Point (MPP) [ $I_{mpp}$ ]	41.5 A
Voltage at Maximum Power Point (MPP) [ $V_{mpp}$ ]	241.6 V
Short Circuit (SC) current [ $I_{sc}$ ]	45.55 A
Open Circuit (OC) voltage [ $V_{oc}$ ]	298.4 V

### Characteristic of PV Module

As per the level of irradiation and temperature, the PV module delivers various amounts of current. The PV module behaves differently depending on the types or sizes of the connected load to it. Such behavior is called the characteristic of the PV module.

When the different load is connected, various current and voltage value levels are described by the PV module's characteristics. When the PV module is under no-load condition, the PV module current will be zero, and the voltage across the PV module is maximum so maximum voltage at zero current is called the open-circuit voltage ( $V_{oc}$ ) of the PV module. When two terminals of the PV module are short-circuited, the maximum current flow at zero voltage through it. It is called short circuit current ( $I_{sc}$ ). The P-V curve and I-V curve is shown in Fig. 5.5. In the P-V curve, the maximum possible power is provided by PV for a single point at environment condition irradiation, and the temperature is called MPP. The value of voltage and current at MPP is known as  $V_{mp}$  and  $I_{mp}$ . The power at MPP is known as  $P_{mp}$ . The  $P_{mp}$  is shown in the I-V curve.

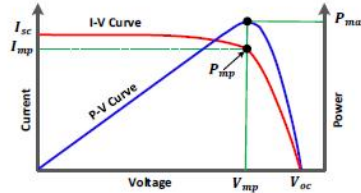


**FIGURE: I-V and P-V curve with MPP**

The performance of the PV module is dependent on its operating conditions. The power is generated from PV, which relies on irradiation and ambient temperature. It is noticed that the output current of the PV module is mainly affected by the change in irradiance. The PV system is designed to operate at a maximum power point (MPP) for any irradiance.

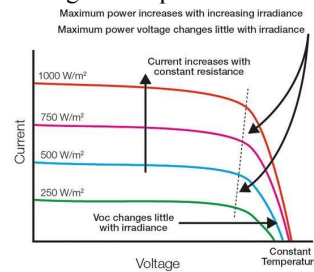


**FIGURE: I-V characteristic at different irradiance level**

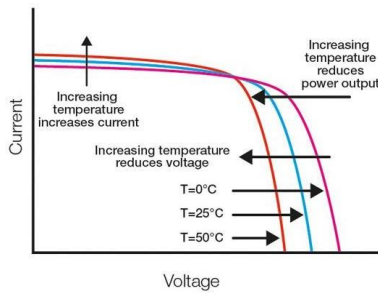


**FIGURE: I-V characteristic at different temperature**

In the power versus voltage curve of a PV module, there is a single maximum of power, i.e., a peak power corresponding to a particular voltage and current. The PV solar system has very low efficiency. The efficiency of the solar cell is approximately 8 to 16%. The solar panel's efficiency is 50 to 40% only. So, the solar panel converts only 50 to 40% electrical power from solar irradiation. So, it is required to operate the module at a peak power point. The load can transfer maximum power under varying irradiation and temperature. The maximized power will help to improve the utilization of the PV solar module. The MPP tracker extracts the maximum energy from the solar PV module and transfers it to load [162]. A DC/DC converter transfers this maximum power to the solar PV module load as an interfacing device. The load impedance is varied by changing the duty cycle and matching the source at the peak power point. Thus, maximum power can transfer it. The intersection of the actual load mismatches the operating point of the ideal and real load. It is shown in Fig. 5.8

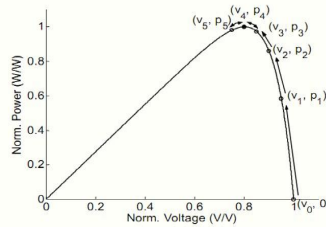
The various algorithms for maximum power point tracking (MPPT) are available as per the literature. There are several existing algorithms for MPPT to maximize output power. The different algorithms for MPPT are as per the following.

- Perturb and observation (P&O)
- Incremental conductance (INC)
- Parasitic capacitance
- Voltage based peak power tracking
- Current based peak power tracking



**Perturbation & Observation (P&O) algorithm for MPPT in PVES:**

The variation of the duty cycle is that the converter's source impedance can match equally to load impedance and peak power. So, various algorithms are available to achieve peak power. The perturbation & Observation (P&O) algorithm is the most use due to its simple implementation. (Kim et al., 1996).



**Flow chart of P&O for MPPT in PVES:**

Fig. 5.10 is present the flow chart of the P&O algorithm. This algorithm observes the array's output power and perturbs the power based on an array voltage increment. This algorithm continuously increments or decreases the reference voltage based on the previous power sample [165].

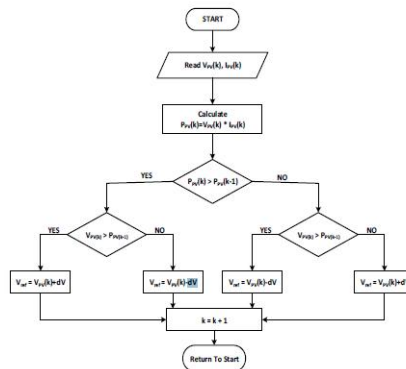


**FIGURE: Flowchart of the P&O algorithm for MPPT in PVES**

Here a reference duty cycle is set corresponding to the peak power point of the module. The value of current and voltage obtain from the solar PV module. From the measured voltage and current, calculate the cost of power. The power and voltage value are store at k instant. Then values are again measured at k-1 instant, and from measured values, calculate the power.

The P&O algorithm has a high steady-state error. The dynamic response will be slow when a small increment value and a low sampling rate are employed. The short increments are essential to decrease the steady-state error because the P&O always makes the operating point oscillate near the MPP but never precisely. When the increment is lower, the system will be closer to the array MPP. The algorithm will work faster in a more significant increment but increase the steady-state error. The small increments tend to make the algorithm more stable and accurate when the operating conditions of the PV array change [164].

**PVES with MPPT Control**

The control diagram of PVES with MPPT is shown in Fig. 5.11. The solar PV module is connected to the DC bus of a hybrid microgrid through the DC-DC boost converter. The output of the solar PV module  $V_{PV}$  and  $I_{PV}$  are continuously measured and supply input to the MPPT. The P&O algorithm tracks the maximum power point and generates the boost converter's duty cycle for MOSFET. The duty cycle is such that the PV module delivers the maximum power, and the output voltage of the boost converter is maintained the constant value. The Simulink model of PVES with MPPT control is shown in Fig. 5.12.

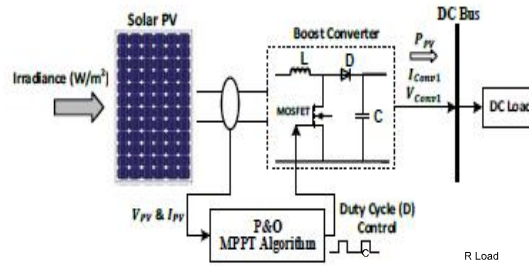


**FIGURE: Diagram of PVES with MPPT control**

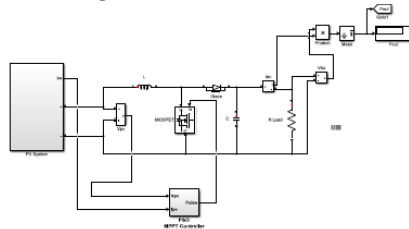


**FIGURE: Simulink model of PVES with MPPT control**

**Result and Discussion**

The PV module's performance and array at different irradiation and temperature determine at Standard Test Condition (STC). The STC is the light intensity at  $1000 \text{ W/m}^2$  and  $25^\circ\text{C}$  temperature of the PV cell. The block diagram, as shown in Fig. 5.2, is simulated using SIMULINK with parameters of Table 5.1. I-V and P-V characteristics at different irradiation levels of the PV module (TGD Holding T250M606) are present in Fig. 5.15 and 5.14. Its current and powers are 8.66 A and 250.66 W, respectively, at irradiation  $1 \text{ KW/m}^2$ . The variation of current in the I-V curve is shown at different irradiation from  $200 \text{ W/m}^2$  to  $1000 \text{ W/m}^2$ .

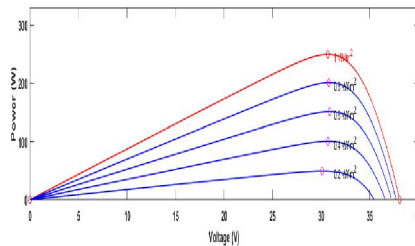


**FIGURE: P-V characteristic of PV module at different irradiation**

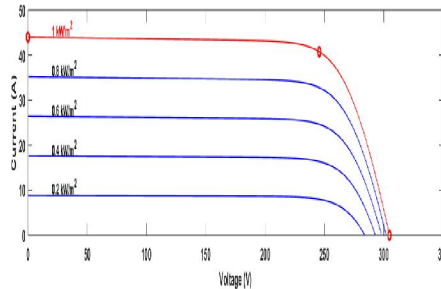


**FIGURE: I-V characteristic of the PV module at different irradiation**

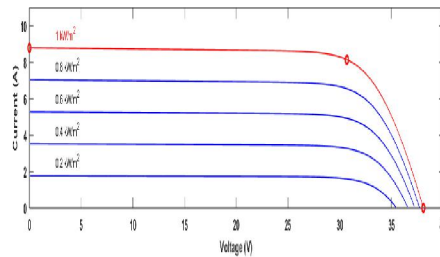


**FIGURE: P-V characteristic of PV array at different irradiation**

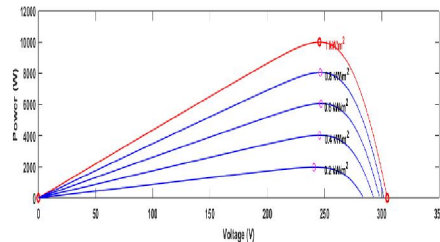


**FIGURE: I-V characteristic of PV array at different irradiation**

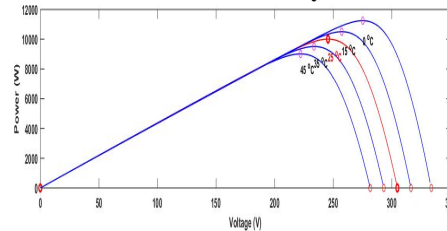


**FIGURE: P-V characteristic of PV array at different temperature**

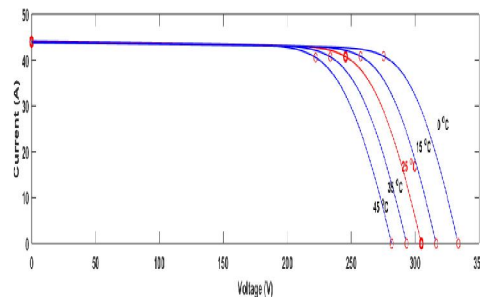


**FIGURE: I-V characteristic of PV array at different temperature**

P-V and I-V characteristics at different irradiation of PV array, respectively. When irradiation increases from 0.25 KW/m<sup>2</sup> to 1 KW/m<sup>2</sup>, the PV array's current and power output also increase. The 10 KW, maximum PV power output is achieved at irradiation of 1000 W/m<sup>2</sup>. P-V and I-V characteristics of the PV array at different temperatures are present in Fig. 5.17 and 5.18, respectively. When the temperature increases from 0° C to 50° C, the current output increment is less compared to the voltage decrement. So, the power output of the PV array reduces more when the increase in temperature. A small circle shows the maximum power point (MPP) at different irradiation in Fig. 5.15. The block diagram, as shown in Fig. 5.11, is simulated using SIMULINK with parameters of Table 5.5. The variation of PV array voltage, current and, power at different irradiance is shown in Table 5.5. The PV converter output is shown in Table 5.4. The duty cycle changes as per variation in PV array output. So, the output of the PV converter maintains at a constant voltage of 400 V.



**TABLE: PV output at MPPT for different irradiance**

Irradiance (W/m <sup>2</sup> )	PV Output		
	V <sub>PV</sub> (V)	I <sub>PV</sub> (A)	P <sub>PV</sub> (W)
200	240.80	8.30	200
400	245.70	16.280	4000
600	246.90	24.30	6000
800	246.20	32.493	8000
1000	245.55	40.724	10000

**TABLE: PV converter output at MPPT for different irradiance**

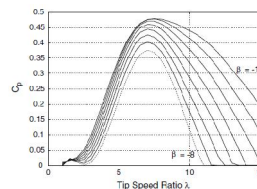
Irradiance (W/m <sup>2</sup> )	DC-DC Converter Output of PV			V <sub>PV</sub> V <sub>DC</sub>	Duty Cycle $D = 1 - \frac{V_{PV}}{V_{DC}}$
	V <sub>DC</sub> (V)	I <sub>DC</sub> (A)	P <sub>Out</sub> (W)		
200	400.18	5.12	2000	0.6017	0.3829
400	400.12	10.32	4000	0.6140	0.3860
600	400.08	15.24	6000	0.6171	0.3829
800	400.04	20.64	8000	0.6154	0.3846
1000	400.01	25.36	10000	0.6138	0.3862

### WIND ENERGY SYSTEM

Wind power generates from wind turbines due to the movement of the wind. The energy related of this wind is called kinetic energy. This kinetic energy ( $E$ ) with mass ( $m$ ) and velocity ( $v$ ) can be expressed [165]

The actual power generated in the wind would be smaller due to friction losses. The power coefficient ( $C_p$ ) is defined as a ratio of actual power to theoretical power. [166]

The power coefficient is varying with the tip speed ratio. The relation between the power coefficient ( $C_p$ ) and TSR is shown in Fig. 3.19 [165]. When wind speed changes, the Modeling and MPPT Control of DG  $C_p$  and TSR will vary. So, the value of  $C_p$  will become maximum at a specific value of TSR. When wind speed is constant,  $C_p$  will be maximum at one speed only. As mentioned earlier, the rotor power coefficient  $C_p$  It depends on the blade pitch angle. Rotating the blade about their long axes will change the pitch angle, modifying  $C_p$ , and thus changing the power is extracted from the wind. The relation between  $C_p$  and TSR at a different pitch angle is shown in Fig. 3.20 for an example of a turbine. Blade-pitching can be achieved precisely and quickly using electric control, allowing smooth control of output power. [166]



**C<sub>p</sub> versus  $\lambda$  at different blade pitch angle ( $\beta$ ) [166]**

### Classification of Wind Energy Conversion Systems

Today wind energy cost is down due to advancement in technology. The different wind generator topology has been analyzed to fit into the system. Today lightweight generators can be surviving the time of amount. The various wind generator systems can be classified on the way of different factors.

The orientation of rotor axis: Vertical or horizontal

Speed: Variable or constant

Power control of rotor: Stall, pitch, and active stall

Position of rotor: Downward or upward tower

Copyright to IJARSCT

DOI: 10.48175/568

[www.ijarsct.co.in](http://www.ijarsct.co.in)

The wind source is natural, which has required some energy conversion system. It fits into an electrical system without disturbing frequency and voltage. The wind turbine topology has mostly classification based on speed and power control. It is classified into four categories. [167]

**Type I: Squirrel Cage Induction Generator (SCIG) based WECS:**

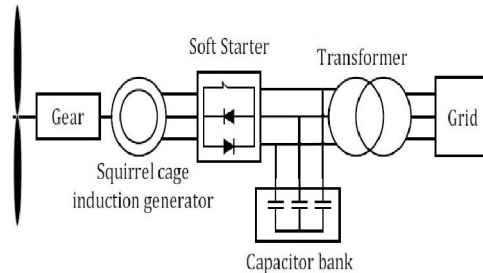


**FIGURE: Type I: SCIG based WECS**

**Type II: Wound Rotor Induction Generator (WRIG) based WECS**

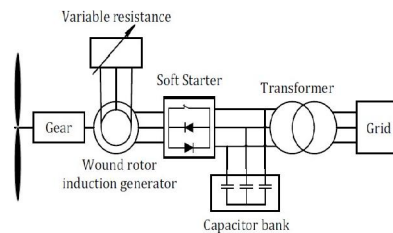
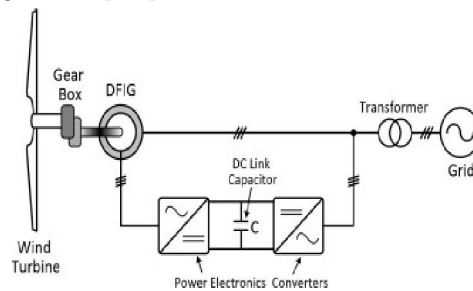


**FIGURE: Type II: WRIG based WECS**

**Type III: Double Fed Induction Generator (DFIG) based WECS**

The double fed induction generator (DFIG) is connected with wind turbines in the type III WECS system. It is shown in Fig. 5.25. The speed of the generator can be changed by varying frequencies produced by the controlled power converter. A generator can be rotated with sub synchronous, super synchronous, and synchronous speed in this system. When the generator is turned at sub synchronous speed, the real power will be injected into the grid. The energy will be absorbed from the grid when the generator is rotated at super synchronous. At synchronous speed, there is no exchange power between the grid and the generator [167].



**Typed IV: Permanent Magnet Synchronous Generator (PMSG) based WECS**

Type IV based WECS system is consists of a permanent magnet synchronous generator (PMSG) and a power converter. The PMSG is a fixed speed synchronous generator that has a large number of poles. PMSG can be connected with load or grid through a rectifier and inverter. In this WECS system, maximum power

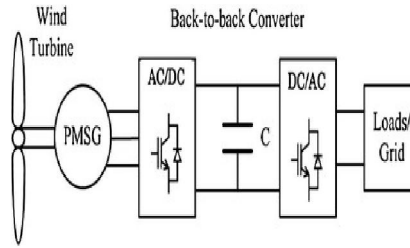


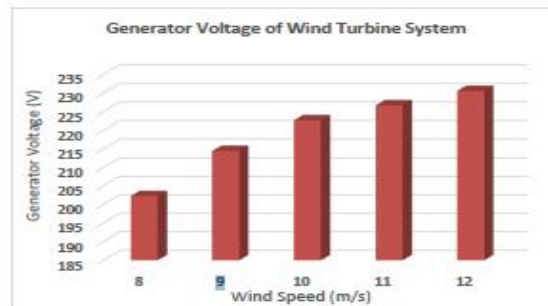
**FIGURE: Type IV: PMSG based WECS**

**Result and Discussion**

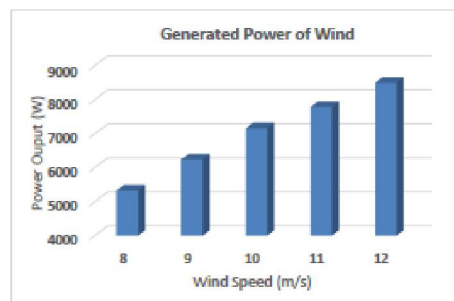
The block diagram, as shown in Fig. 5.29, is simulated using SIMULINK with parameters of Table 3.5. Analysis of the P&O algorithm's sensitivity is tested by different wind speed between 8 to 12 m/s to determine the effect of change in the parameter value. The simulation result of the wind generator output at different wind speed is shown in Table 5.6. The voltage **V<sub>w</sub>**, current **I<sub>w</sub>** and power **P<sub>w</sub>** of wind generator are found at a wind speed of 8 to 12 m/s. From the simulation result, it can be seen that sufficient output voltage and power are generated at higher wind speed.

**TABLE: Wind generator output at different wind speed**

Wind Speed (m/s)	Wind Generator Output		
	V <sub>w</sub> (V)	I <sub>w</sub> (A)	P <sub>w</sub> (W)
8	198.31	26.091	5330.78
9	214.45	29.101	6240.92
10	222.68	32.156	7160.56
11	226.71	34.350	7787.66
12	230.55	36.863	8498.80



**(a)**



**(b)**

**FIGURE: Generated output of wind turbine: (a) Voltage (b) Power**

The converter output of wind generator at different wind speed is shown in Fig. 5.30. The variation of wind speed will change the duty cycle. The DC bus voltage is 400 V. So, the voltage output (**V<sub>DC</sub>**) of the DC-DC converter is maintained at a constant of 400 V. The wind generator output (**V<sub>w</sub>**) is 250 V. When wind speed increases, **V<sub>w</sub>** is also

raised. So, the duty cycle of the converter is reduced to maintained DC bus voltage. The duty cycle at different wind speed is found in Table 5.7. The variation of the duty cycle for a converter at different wind speed is shown in Fig. 5.31.

**TABLE: Wind generator converter output at different wind speed for MPPT**

Wind Speed (m/s)	DC-DC Converter output of wind generator			$\frac{V_w}{V_{DC}}$	Duty Cycle $D = 1 - \frac{V_w}{V_{DC}}$
	$V_{DC}$ (V)	$I_{DC}$ (A)	$P_{Out}$ (W)		
8	399.98	13.327	5330.78	0.496	0.50
9	400.01	15.602	6240.92	0.536	0.46
10	400.08	17.897	7160.56	0.557	0.44
11	400.03	19.467	7787.66	0.567	0.43
12	400.06	21.243	8498.80	0.576	0.42

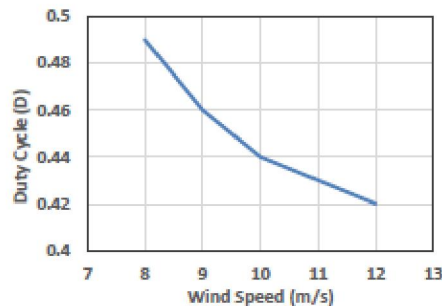


**FIGURE: Variation of duty cycle at different wind speed for MPPT control**

**ENERGY STORAGE SYSTEM**

An energy storage system (ESS) is used where power electronics converters are required to connect various energy types. ESS is essential in a hybrid microgrid for power management in case of a sudden change in load, change in atmospheric condition, etc. Today there are various types of energy storage devices used in a hybrid microgrid.

Electrochemical energy storage device: Battery energy storage system (BESS) and Electrochemical capacitors (ECs)

Mechanical energy storage: Flywheel energy storage systems (FESS), Pump hydro (PH), and compressed air energy storage (CAES)

Electromagnetic energy storage: Superconducting magnetic energy storage (SMES)

Classification of ESS as per power density is shown in Fig. 5.52.

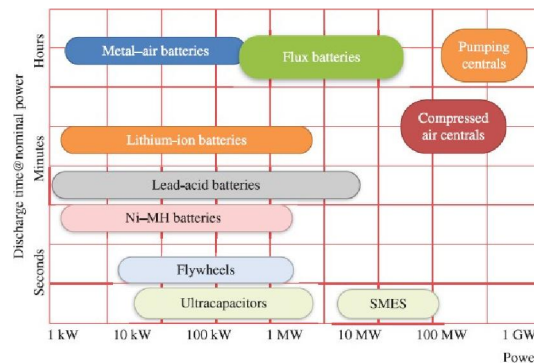


**FIGURE: Classification of ES as per power density**

### Battery Energy Storage System

Today, the battery energy storage system (BESS) is a significant energy storage device to manage the power balance between load and variable renewable sources such as solar and wind. Its electrochemical energy source is used in the hybrid system, which provides higher energy and power capability.

Today a different type of battery is available in the market.

- Nickel Cadmium (NiCd)
- Nickel-Metal Hydride (NiMH)
- Lead Acid (Pb-acid)
- Lithium-Ion (Li-ion)
- Lithium Polymer (Li-poly)
- Sodium Sulphur
- Sodium Nickel Chloride
- Zinc-air

### IV. SUMMARY

Section 5.1 presents the modeling of the PV source and its MPPT control with PVES. The MPPT control helps the utilization of PV power at low irradiance. The P&O algorithm for MPPT is implemented. The effectiveness of MPPT with PVES is evaluated through MATLAB/Simulink at different solar irradiance. Section 5.2 presents the WES, modeling of PMSG, and its MPPT control. The simulation result is found at variation in wind speed for MPPT control in WES. The simulation result of PVES and WES shows that the DC bus output voltage in a hybrid microgrid is maintained constant at variable irradiance and wind speed by the change in a duty cycle of the DC-DC boost converter. Section 5.5 presents the ESS, modeling of battery, and SOC Estimation. In this chapter, the modeling of the DG unit and its MPPT control was analysed. The next chapter focuses on droop control of the DG unit in a hybrid microgrid.

### V. CONCLUSION

**Simulation Tool Overview:** SKM and Homer are widely recognized simulation tools used in the field of electrical engineering and renewable energy. SKM (short for ETAP - Electrical Transient Analyzer Program) is used for analyzing power systems, including microgrids, to ensure stability, reliability, and optimal performance under different operating conditions. On the other hand, Homer (Hybrid Optimization Model for Electric Renewables) is specifically designed for optimizing the integration of renewable energy sources like solar and biomass into microgrid systems. It helps in designing and sizing components such as solar panels, batteries, inverters, and generators to meet specific load requirements while considering factors like resource availability, economics, and system reliability.

- **Scenario Analysis:** The chapter discusses various scenarios simulated using SKM and Homer. These scenarios include:
- **Baseline Simulation:** Analyzing the microgrid's performance without any control or optimization techniques to establish a baseline for comparison.
- **Optimized Control Simulation:** Implementing the real-time power management system (RPMS) based on non-cooperative game theory for load scheduling, generation control, and distribution management. This simulation aims to demonstrate how optimization techniques improve stability, reliability, and economic efficiency of the microgrid.
- **Impact of Renewable Integration:** Evaluating the impact of integrating renewable energy sources (solar PV and biogas) on overall system performance, including energy generation, load management, and grid stability.
- **Performance Metrics:** The characteristics of the isolated hybrid microgrid are evaluated based on several performance metrics, such as:
- **Stability:** Assessing the ability of the microgrid to maintain stable voltage and frequency levels under varying load and generation conditions.
- **Reliability:** Measuring the system's reliability in providing continuous and uninterrupted electricity supply to the connected loads.



**REFERENCES**

- [1] Debajit Palit, Arvind Garimella, Martand Shardul, and Saswata Chaudhury, "Analysis of the electrification programme in India using the 'Energyplus' framework and the key lessons," Final report 2015 GNESD, TERI, 2015, pp. 1-83.
- [2] Abhishek Jain, Sudatta Ray, Karthik Ganesh, Michale Aklin, Chao-yo Cheng, and Johannes Urpelainen, "Access to clean cooking Energy and Electricity Survey of States," CEEW Report - 2015, pp. 1-65.
- [3] Rajkiran Bilolikar & Ravi Deshmukh, "Rural Electrification in India - an overview," National Power Training Institute, 2014, pp. 1-12.
- [4] Maximo Torero, "The impact of Rural Electrification challenges and ways forward," 11th conference AFD Proparco/EudN: Energy for Development No. 16, 2014, pp. 1-34.
- [5] Johannes Urpelainen, "Energy poverty and perceptions of solar power in marginalized communities: Survey evidence from Uttar Pradesh, India," Elsevier Journal on Renewable Energy, Volume 85, January 2016, pp. 534-539.
- [6] Dr. Pradeepta Kumar Samanta, "A study of Rural Electrification Infrastructure in India," IOSR Journal of Business and Management, Vol. 17, issue 2, Ver IV, February 2015, pp. 54-59.
- [7] Supriya Ray, Biswajit Ghosh, Suchandra Bardhan, Bidyut Battacharya, "Studies on the impact of energy Quality on Human Development Index," Elsevier Journal on Renewable Energy, Vol. 92, July 2016, pp. 117-126.
- [8] D. Salomonsson and A. Sannino, "Low-voltage dc distribution system for commercial power systems with sensitive electronic loads," IEEE Trans. Pow. Del., vol. 22, no. 3, July 2007, pp. 1620-1627.
- [9] W. Lu and B. T. Ooi, "Optimal acquisition and aggregation of offshore wind power by multiterminal voltage-source HVDC," IEEE Trans. Power Del., vol. 18, no. 1, Jan 2003, pp. 201-206.
- [10] Antimo Barbato and Antonio Capone, "Optimization models and methods for demand side management of residential users: a survey," MDPI journal Energies, vol. 7, Sept 2014, pp. 5787-5824.
- [11] Linas Gelazanskas, Kelum A. A. Gamage, "Demand side management in smart grid: a review and proposal for future utilization," Elsevier journal of sustainable cities and society, No. 11, 2014, pp. 22-30.
- [12] Zhou Wu, Henerica Tazvinga, Xiaohu Xia, "Demand side management of photovoltaic-battery hybrid system," Elsevier journal of Applied Energy, No. 148, April 2015, pp. 294-304.
- [13] T.R. Ayodele, A.S.O. Ogunjuyigbe, K.O. Akpeji, O.O. Akinola, "Prioritized rule based load management technique for residential building powered by PV/battery system," Elsevier journal of Engineering Science and Technology, an international journal, No. 20, April 2017, pp. 859-873.
- [14] S. Rauf, S. Rasool, M. Rizwan, M. Yousaf, N. Khan, "Domestic electrical load management using smart grid," Elsevier Energy Procedia, No. 100, September 2016, pp. 253-260.
- [15] C. Wimpler, G. Hejazi, E. de Oliveira Fernandes, C. Moreira, S. Connors, "Impact of Load Shifting on Renewable Energy Integration," Elsevier Energy Procedia, No. 107, September 2017, pp. 248-252.
- [16] Solene Goy, Araz Ashouri, Francois Marechal, Donal Finn, "Estimating the potential for thermal load management in buildings at a large scale: overcoming challenges towards a replicable methodology," Elsevier Energy Procedia, Vol. 111, 2017, pp. 740-749.
- [17] Ralf Boehm, Joerg Franke, "Demand side management by flexible generation of compressed air," Elsevier Procedia CIRP, Vol. 63, 2017, pp. 195-200.
- [18] M.H. Alham, M. Elshahed, Doaa Khalil Ibrahim, Essam El Din Abo ElZahab, "Optimal operation of power system incorporating wind energy with demand side management," Elsevier Journal of Ain Shams Engineering Journal, Vol. 8, issue 1, March 2017, pp. 1-7.
- [19] Xing ping Zhang, Kaiyan Luo, Qinliang Tan, "A game theory analysis of China's agri-biomass based power generation supply chain: A co-opetition strategy," Elsevier Energy Procedia 105, March 2017, pp. 168-173.
- [20] Faycal Elatrech Kratima, Fatima Zohra Gherbi, and Fatiha Lakdja, "Application of cooperative game theory in power system allocation problems," Leonardo Journal of Science, Issue 3, July 2013, pp. 125-136.